is ~0.35 V (see Table IV). While the lack of $E_{1/2}$ values obviates calculation of ΔE_0 for electron transfer between $Ir(P(OPh)_3)_2(mnt)^-$ and MV^{2+}, we can estimate that for this system ΔE_0 is ~-0.1 v based on the fact that the slightly more reducing complex $Ir(CO)(PPh_3)(mnt)^-$ produces partial reduction of MV^{2+} thermally. The error on this estimate of ΔE_0 is sizable but leads to only small changes in the reorganization energy estimated by using eq 1.

The reorganization energy λ obtained by using E_{op} of 532 nm and ΔE_0 of -0.1 V is 56 kcal/mol. While λ is a composite of several terms, the two dominant ones are the individual reorganization energies of the reaction components. From the self-exchange rate constant for $MV^{2+/+\cdot}$,[7c,32] it is possible to estimate $\lambda(MV^{2+})$ as 12-16 kcal/mol, leaving λ for the Ir(I/II) couple in this system as 40-44 kcal/mol. This value is consistent with the notion of a large reorganization energy in the oxidation of these $IrLL'(mnt)^{n-}$ systems.

Conclusions. The results presented here show that as ligand donor ability is changed in the $IrLL'(mnt)^{n-}$ system, the reducing ability of the complex is systematically altered. This reveals itself by different electron-transfer behavior with the acceptor molecule MV^{2+}. The most reducing complex, $Ir(CO)(CN)(mnt)^{2-}$, reduces MV^{2+} quantitatively by thermal electron transfer while the least reducing complex, $Ir(CO)_2(mnt)^-$, exhibits only an optical-charge-transfer band without formation of free $MV^{+\cdot}$. The complexes $Ir(CO)(PPh_3)(mnt)^-$ and $Ir(P(OPh)_3)_2(mnt)^-$ show intermediate behavior with photoassisted and photoinduced electron transfer, respectively. From E_{op} of the last of these complexes with MV^{2+}, it is possible to estimate the reorganization energy of the Ir(I/II) couple in this complex as 40-44 kcal/mol. The X-ray structural results show that oxidation of $Ir(CO)(P(p\text{-tol})_3)(mnt)^-$ leads to dimerization and a structure containing an Ir-Ir single bond with a coordination geometry for Ir(II) that is strikingly different from the square-planar arrangement usually seen for Ir(I).

Acknowledgment. We wish to thank the National Science Foundation (Grant CHE 86-03055) for support of this work, and the Johnson Matthey Co., Inc., for a generous loan of iridium salts. We also wish to acknowledge assistance from Dr. Gordon S. Miller in early stages of this work and helpful discussions with Prof. George McLendon.

Supplementary Material Available: Table SI (complete crystal data and intensity collection parameters for the structure determinations of **5** and **6b**), Tables SII and SIII (refined thermal parameters and calculated hydrogen positional parameters for **5**), Tables SIV-SVII (refined thermal parameters, calculated hydrogen positional parameters, and complete bond distances and angles for **6b**), and Figure S1 (crystal structure packing for **6b**) (15 pages); tables of observed and calculated structure factor amplitudes (×10) for **5** and **6b** (44 pages). Ordering information is given on any current masthead page.

(32) Bock, C. R.; Connor, J. A.; Gutierrez, A. R.; Meyer, T. J.; Whitten, D. G.; Sullivan, B. P.; Nagle, J. K. *Chem. Phys. Lett.* **1979**, *61*, 522.

Contribution from the Departments of Chemistry, Indiana University, Bloomington, Indiana 47405, and University of Oslo, Blindern, N-0315, Oslo 3, Norway

Structure and Reactivity of $Cr(OCMe_3)_4$

Eric G. Thaler,[†] Kristin Rypdal,[‡] Arne Haaland,*[,‡] and Kenneth G. Caulton*[,†]

Received October 20, 1988

$Cr(O^tBu)_4$ has been characterized by ^1H NMR and magnetic susceptibility methods, and the structure has been determined in the gas phase. The gas-phase electron diffraction pattern recorded with a nozzle temperature of about 130 °C is consistent with a model of S_4 symmetry. The most important structural parameters are Cr-O = 175.1 (7) pm, O-C = 141.1 (12) pm, and C-C = 151.7 (7) pm and ∠CrOC = 142 (2)° and ∠OCC = 107.8 (4)°. No evidence is found for deviation from tetrahedral valence angles at Cr. $Cr(O^tBu)_4$, in which chromium is completely shielded by a hydrocarbon exterior, shows no tendency to add the Lewis bases PMe_2Ph, PPh_2H, MeCN, MeNC, or CO but oxidizes $LiPPh_2$ to Ph_2PPPh_2, with production of $LiCr(O^tBu)_4$. Several one-electron redox reagents containing open coordination sites will interconvert $Cr(O^tBu)_4^-$ and $Cr(O^tBu)_4$, with evidence that each proceeds by an inner-sphere mechanism.

Introduction

$Cr(O^tBu)_4$ was initially reported by Hagihara and co-workers in 1959 and was the first monomeric Cr(IV) species supported solely by organic ligands.[1] Its synthesis was somewhat unique for metal alkoxides in that it may be considered formally as an oxidative addition of 2 equiv of di-*tert*-butyl peroxide to the Cr^0 metal center of bis(benzene)chromium. This first report was followed by the report of several alternative synthetic routes to $Cr(O^tBu)_4$,[2] a brief summary of some of its reaction chemistry (which emphasized proton-transfer reactions),[3] and a report on the thermodynamics of this compound.[4] Characterization of $Cr(O^tBu)_4$ includes solid-state magnetic susceptibility measurements, elemental analysis, and a cryoscopic molecular weight determination. Infrared, electronic, and ESR spectra were consistent with the compound having approximate T_d symmetry in solution. However, band splitting in the ligand field spectrum was interpreted as evidence for a distortion from tetrahedral symmetry to D_{2d}. Due to the high volatility of this compound, we felt that a more exact structural characterization could be accomplished through a gas-phase electron diffraction study, where the $Cr(O^tBu)_4$ molecules would be devoid of the solvent interactions possible in solution spectral studies, and no crystal packing forces would be present, as can be the case in X-ray structural analysis. We report here the results of such a study and present some of the reactivity trends for $Cr(O^tBu)_4$.

Experimental Section

General Procedures. All operations were performed under N_2 (unless specifically stated otherwise) by using standard Schlenk techniques for handling air- and moisture-sensitive materials. Tetrahydrofuran, benzene, and toluene were all dried and distilled prior to use from solutions containing sodium/potassium benzophenone ketyl. "Ultra-high-purity" grade hydrogen and carbon monoxide gases were purchased from Air Products. Copper(I) chloride was synthesized by literature methods,[5] as was $CrCl_3(THF)_3$.[6]

[†] Indiana University.
[‡] University of Oslo.

(1) Hagihara, M.; Yamasaki, H. *J. Am. Chem. Soc.* **1959**, *81*, 3160.
(2) Basi, J. S.; Bradley, D. C. *Proc. Chem. Soc.* **1963**, 305. Krauss, H. L.; Munster, G. *Z. Anorg. Allg. Chem.* **1967**, *24*, 352. Alyea, E. C.; Basi, J. S.; Bradley, D. C.; Chisholm, M. H. *Chem. Commun.* **1968**, 495.
(3) Alyea, E. C.; Basi, J. S.; Bradley, D. C.; Chisholm, M. H. *J. Chem. Soc.* **1971**, 772.
(4) Bradley, D. C.; Hillyer, M. J. *Trans. Faraday Soc.* **1966**, *62*, 2382.
(5) *Inorg. Synth.* **1946**, *2*, 1.
(6) Herwig, W.; Zeiss, H. H. *J. Org. Chem.* **1958**, *23*, 1404.

0020-1669/89/1328-2431$01.50/0

$Cr(O^tBu)_4$. In a typical preparation, KO^tBu (2.398 g; 21.4 mmol) suspended in THF (20 mL) was added to a slurry of $CrCl_3(THF)_3$ (2.0 g; 5.3 mmol) in THF, followed by the addition of CuCl (0.57 g; 5.3 mmol). The reaction mixture was then stirred for 18 h to yield a red-brown precipitate and a deep blue solution. Insolubles were removed by filtering through a pad of filter-aid packed on a medium-porosity frit. The THF was then removed in vacuo, and the remaining blue gum was distilled under dynamic vacuum ($\sim 5 \times 10^{-3}$ Torr) between 68 and 70 °C, yielding pure $Cr(O^tBu)_4$.[7] Yield: 1.24 g; 67%. ^1H NMR (C_6D_6): δ = 3 ppm (br). IR (Nujol): 1370 s, 1240 s, 1180 vs, 1035 w, 950 vs, 795 s, 630 s, 480 m, 397 m cm^{-1}. Magnetic moment[8] (23 °C; C_6D_6): μ = 2.86 μ_B.

Reactivity Studies. $Cr(O^tBu)_4$ and PMe_2Ph/H_2 (Ph = Phenyl). $Cr(O^tBu)_4$ (0.5 g; 1.45 mmol) and PMe_2Ph (0.8 g; 5.8 mmol) were placed in benzene (10 mL) and then transferred to an autoclave, which was subsequently charged with H_2 (2100 psi). The reaction mixture was stirred for 24 h, after which time only $Cr(O^tBu)_4$ and PMe_2Ph were recovered.

$Cr(O^tBu)_4$ and CH_3NC. $Cr(O^tBu)_4$ (0.15 g; 0.44 mmol) was placed in toluene (10 mL), and CH_3NC (0.069 mL; 0.6 mmol) was added by means of a microliter syringe. The solution was refluxed for 18 h, after which time the $Cr(O^tBu)_4$ was recovered.

$Cr(O^tBu)_4$ and PPh_2H. The attempted reaction was carried out in the same manner as with CH_3NC using THF in place of toluene. No reaction occurred.

$Cr(O^tBu)_4$ and $LiPPh_2$. $LiPPh_2$ (1 equiv) in THF (5 mL) was added to $Cr(O^tBu)_4$ (1.27 g; 3.69 mmol) in THF (20 mL). The reaction mixture was stirred for 1 h to yield a bright purple precipitate ($LiCr(O^tBu)_4$) and a light blue solution containing $Cr(O^tBu)_4$ (^1H NMR (C_6D_6): δ = 3 ppm) and P_2Ph_4 (^{31}P NMR (C_6D_6): δ = 14.3 ppm). The identity of $LiCr(O^tBu)_4$ was verified by its conversion to $Cr(O^tBu)_4$ using 1 equiv of CuCl.

$Cr(O^tBu)_4$ and Cp_2Co. $Cr(O^tBu)_4$ (0.2 g; 0.58 mmol) and Cp_2Co (0.2 g; 1.16 mmol) were placed in benzene (20 mL) and refluxed for 9 h, after which time the solvent was removed in vacuo. The remaining dark solid was dissolved in C_6D_6. ^1H NMR gave only two broad resonances, δ = 3 ppm ($Cr(O^tBu)_4$) and δ = −51 ppm (Cp_2Co).

$Cr(O^tBu)_4$ and CO. $Cr(O^tBu)_4$ (0.16 g; 0.46 mmol) in benzene (10 mL) was placed in a low-pressure reaction tube, which was then charged with 30-psi CO. The solution was then allowed to stir for 24 h with no noticeable change. The solvent was then removed and the blue $Cr(O^tCu)_4$ recovered. ^1H NMR: δ = 3 ppm.

Electron Diffraction. The gas-phase electron diffraction pattern of $Cr(OMe_3)_4$ was recorded on Balzers Eldigraph KDG-2 with nozzle and reservoir temperatures of approximately 130 °C. Exposures were made with nozzle-to-plate distances of 50 and 25 cm; five plates for each distance were used in this study. Atomic scattering factors were taken from ref 9. Average modified molecular intensity curves ranged from s = 30.00 to 147.50 nm^{-1} with increment 1.25 nm^{-1} (50 cm) and from s = 35.00 to 210.00 nm^{-1} with increment 2.50 nm^{-1} (25 cm).

Structure Refinements. If the valence angles at oxygen are less than 180°, the complete description of the structure of a $Cr(OCMe_3)_4$ molecule requires specification of eight dihedral angles, four describing torsion around Cr–O bonds, four describing torsion around O–C bonds. Exploratory least-squares refinements showed that satisfactory agreement between experimental and calculated intensities could only be obtained if all these dihedral angles were about 180°, i.e., if each of the four $O_3CrOCMe_3$ fragments were in or near an extended anti-anti conformation:

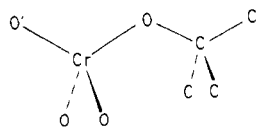

The highest possible molecular symmetry is then D_{2d} followed by S_4 and D_2. The only model of D_{2d} symmetry, where ϕ(O'CrOC) and seven other dihedral angles are exactly 180°, is shown in Figure 1A. This model may be relaxed to S_4 or D_2 by allowing the dihedral angles to deviate from exactly 180°. The D_2 model thus obtained is the only D_2 model with extended $O_3CrOCMe_3$ fragments, but there is another S_4 model with extended fragments, which can be obtained by rotating all CMe_3 groups approximately 120° about the Cr–O bonds. This model, in which O–C is anti Cr–O''' rather than Cr–O', is shown in Figure 1B,C.

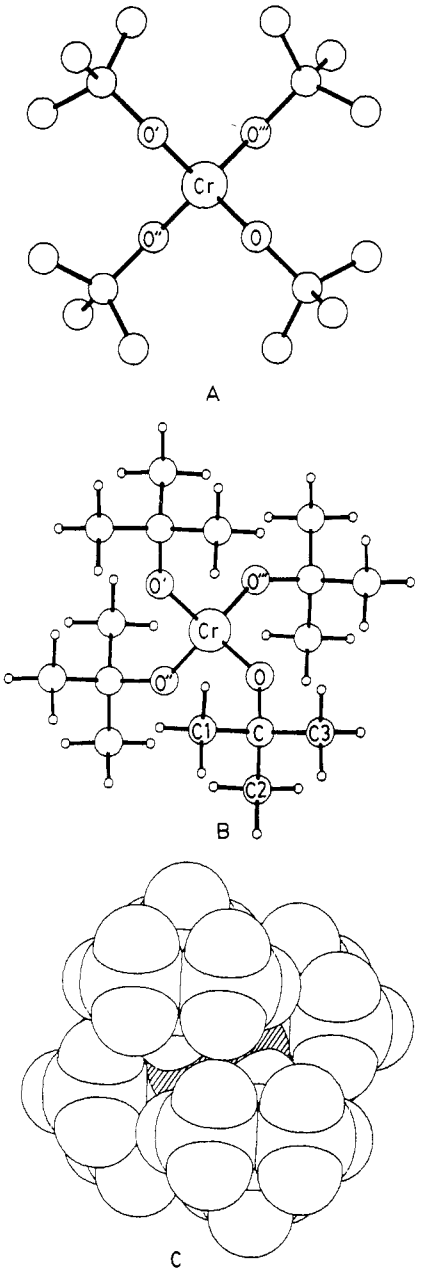

Figure 1. Molecular models of $Cr(OCMe_3)_4$ viewed with down the S_4 symmetry axis: (A) D_{2d} model (H atoms deleted); (B) S_4 model; (C) space-filling drawing of the gas-phase structure (van der Waals radii: H, 120 pm; O, 140 pm; C, 160 pm; Cr (shaded), 200 pm).

Neither the D_{2d} model in Figure 1A nor the relaxed S_4 or D_2 model obtained from it by allowing dihedral angles to deviate from 180° could be brought into satisfactory agreement with the electron diffraction data.

We now turn our attention to the S_4 model shown in Figure 1B,C. It was assumed the CCH_3 fragments have C_{3v} symmetry and that methyl groups are staggered with respect to the bonds radiating from the quaternary C atom. The CMe_3 fragments were likewise assumed to have C_{3v} symmetry. Exploratory refinements were carried out on models with "tilt", i.e., models in which the angle between the 3-fold axis and the O–C bond was treated as an independent variable. When it was found that introduction of this parameter failed to improve the fit, it was fixed at zero in subsequent refinements. The S_4 model is then described by four bond distances (Cr–O, O–C, C–C, and C–H), four valence angles ($\angle$OCrO', $\angle$CrOC, $\angle$OCC, and $\angle$CCH), and the two dihedral angles ϕ(O'CrOC) and ϕ(CrOCC(2)). Least-squares refinements of these 10 structural parameters and 10 rms amplitudes of vibration led to satisfactory agreement between experimental and calculated intensity curves; R = 5.41%. The best parameter values are listed in Table I. Figure 1C shows the van der Waals contours of the final structural model. Experimental and calculated radial distribution curves are compared in Figure 2.

(7) Excessive heating results in thermal decomposition.
(8) Evans, D. F. *J. Chem. Soc.* **1959**, 2003. Kennedy, M. B.; Lisler, M. W.; Marson, R.; Poyntz, R. B. *Can. J. Chem.* **1973**, *51*, 674.
(9) Schäfer, L.; Yates, A. C.; Bonham, R. A. *J. Chem. Phys.* **1971**, *55*, 3055.

Table I. Internuclear Distances (r_a), Vibrational Amplitudes (l), Valence Angles, and Dihedral Angles of $Cr(OCMe_3)_4$[a]

	r_a/pm or angle/deg	l/pm
	Bond Distances	
Cr–O	175.1 (7)	6.5 (4)
O–C	141.1 (12)	6.6 (10)
C–C	151.7 (7)	4.4 (16)
C–H	109.4 (6)	6.9 (10)
	Nonbonded Distances	
Cr···C	298.7 (10)	7.4 (16)
Cr···C(1)	342.1 (12)	14.5 (13)
Cr···C(2)	357.8 (25)	39 (13)
Cr···C(3)	410.9 (8)	12.8 (13)
O···O′	290 (5)	[11.0][b]
O···O″	284 (3)	[11.0][b]
O···C(1)	236.5 (9)	10.7 (10)
C(1)···C(2)	250.2 (10)	4.7 (16)
	Valence Angles	
CrOC	142 (2)	
OCC	107.8 (4)	
CCH	109.4 (13)	
OCrO′	112 (3)	
	Dihedral Angles	
ϕ(O′CrOC)	43 (3)	
ϕ(CrOCC(2))	48 (3)	

[a] Molecular symmetry S_4. Estimated esd's in parentheses in units of the last figure. [b] This value was fixed in the last refinement.

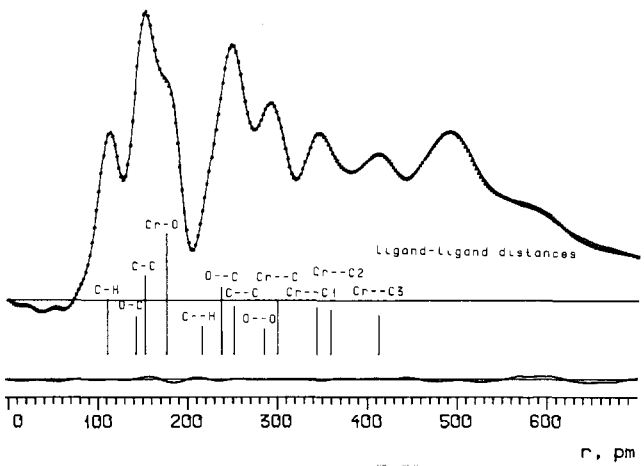

Figure 2. Experimental (···) and calculated (—) radial distribution curves for $Cr(OCMe_3)_4$). Artificial damping constant $k = 3 \times 10^{-7}$ nm^2. Below: difference curve.

Results and Discussion

Synthesis and Characterization. $Cr(O^tBu)_4$ was synthesized by a one-pot procedure summarized in eq 1. This highly volatile

$$4KO^tBu + CrCl_3(THF)_3 + CuCl \xrightarrow{THF} Cr(O^tBu)_4 + Cu^0 + 4KCl \quad (1)$$

product may be purified by vacuum distillation (70 °C, 5×10^{-3} Torr) after filtration from solid products and vacuum removal of solvent at 25 °C. If the reaction is executed in the absence of the one-electron oxidant CuCl, the majority of the chromium is found as an insoluble light blue solid, presumably $KCr(O^tBu)_4$ with a polymeric structure. Numerous attempts to obtain pure crystalline samples of this material by using dioxane or $MeOC_2H_4OMe$ solvent, even in the presence of $Me_2NC_2H_4NMe_2$, were unsuccessful.

$Cr(O^tBu)_4$ is readily identified by its volatility and intense blue color. More quantitatively, it shows a single ^{1}H NMR signal at 3 ppm (full width at half-maximum = 230 Hz) in C_6D_6. This is remarkably close to the chemical shift of O^{t}Bu protons in diamagnetic compounds and indicates localization of unpaired spin density at the metal in $Cr(O^tBu)_4$. A determination of the magnetic susceptibility of $Cr(O^tBu)_4$ in C_6D_6 solution at 23 °C by the Evans method[8] gave a value of $\mu = 2.86\ \mu_B$, indicative of two unpaired electrons for this d^2 metal complex, and thus an orbitally degenerate ground state.

Molecular Structure. The gas-phase electron diffraction pattern recorded with a nozzle temperature of 130 °C was consistent with the S_4 model drawn in Figure 1B,C, but not with the D_{2d} model shown in Figure 1A.

The molecular structure of $Cr(O^tBu)_4$ (I) appears to be closely related to that of $Cr[OCH(CMe_3)_2]_4$ (II), which has been studied by X-ray crystallography.[10] The latter occupies crystal sites of C_2 symmetry, but the molecular symmetry is close to S_4. The two crystallographically independent ∠OCrO angles in II are 110.3 (2) and 112.4 (2)° corresponding to a very slightly flattened O_4 tetrahedron. The best value for the corresponding angle in I is 112°, but the esd indicates a possible range of at least ±6°. Other bond distances and valence angles in the two compounds are Cr–O = 175.1 (2) pm in I vs 177.1 (3) and 177.4 (3) pm in II, O–C = 141.1 (12) pm in I vs 143.3 (6) and 143.1 (5) pm in II, and ∠CrOC = 142 (2)° in I vs 141.1 (2) and 140.5 (2)° in II.

A second, relevant comparison compound, $Cr(CH_2CMe_2Ph)_4$, has much longer metal–ligand distances[11] (Cr–C = 201–205 pm). Ligand–ligand repulsions are therefore not as acute as in $Cr(O^tBu)_4$. Angles Cr–C–C are however smaller (at 119–126°) than the Cr–O–C angles in $Cr(O^tBu)_4$. The first coordination sphere in this molecule is quite close to tetrahedral (C–Cr–C angles = 105–117°). It is of interest that the rotational conformations about the Cr–C bonds are such as to yield a close approximation to S_4 symmetry, as also found in $Cr(O^tBu)_4$.

The difference between the single-bond covalent radii of C (77 pm) and O (66 pm) is 11 pm. The difference between the Cr–O distance in $Cr(O^tBu)_4$, 175 pm, and the Cr–C distance in $Cr(CH_2CMe_2Ph)_4$, 203 pm, is far larger than the difference in single-bond radii. This indicates significant Cr/O double-bond character due to π-donation by oxygen lone pairs.

Internuclear distances indicate that Cr is able to accommodate the four $OCMe_3$ ligands without congestion: the two gauche distances O′···C and O″···C are between 350 and 360 pm; all other interligand O···C distances are greater. All interligand C···C distances are greater than 400 pm.

The ligands appear to clothe the metal atom both comfortably and *well*: In Figure 1C, we present a view of the molecule where the ligand atoms are drawn with van der Waals radii. The Cr atom, which has been drawn with a radius of 200 pm, is barely visible. The effective shielding of the metal atom, the spherical shape, and the nonpolar hydrocarbon exterior readily account for the volatility of $Cr(O^tBu)_4$.

Reactivity. $Cr(O^tBu)_4$ shows no tendency to react with Lewis bases in THF, benzene, or toluene. Thus, 4 equiv of PMe_2Ph give no change in the ^{1}H NMR of either reagent. Addition of even the slender reagents MeCN, MeNC, or CO (2 atm) gives no color change. Attempts at hydrogenolysis in benzene with 100-atm H_2 (in the presence of 4 equiv of PMe_2Ph, to stabilize a product like $H_4Cr(PMe_2Ph)_4$) resulted in recovery of $Cr(O^tBu)_4$. The secondary phosphine PPh_2H was next employed either to coordinate to $Cr(O^tBu)_4$ or even to form Cr–PPh_2 bonds and ^{t}BuOH. After 24 h at reflux temperature in THF, $Cr(O^tBu)_4$ and PPh_2H were recovered (^{31}P NMR evidence). This result (eq 2) shows $Cr(O^tBu)_4$ to be a kinetically ineffective oxidant.

$$Cr(O^tBu)_4 + PPh_2H \not\rightarrow Cr(O^tBu)_3 + {}^tBuOH + \tfrac{1}{2}Ph_2PPPh_2 \quad (2)$$

An observation closely related to eq 2 begins to make clear that it is electron transfer, and not Lewis base addition, which is the characteristic reactivity pattern of $Cr(O^tBu)_4$. Equation 3 reveals electron transfer from PPh_2^- to Cr^{IV}. The Ph_2PPPh_2 (identified

(10) Bochmann, M.; Wilkinson, G.; Yang, G. B.; Hursthouse, M. B.; Malik, K. M. A. *J. Chem. Soc., Dalton Trans.* **1980**, 1863.
(11) Gramlich, V.; Pfferkorn, K. *J. Organomet. Chem.* **1973**, *61*, 247.

$$Cr(O^tBu)_4 + LiPPh_2 \xrightarrow{THF} LiCr(O^tBu)_4 + \tfrac{1}{2}Ph_2PPPh_2 \quad (3)$$

by ^{31}P NMR spectroscopy) is the only phosphorus-containing product. $LiCr(O^tBu)_4$, also insoluble (cf. $KCr(O^tBu)_4$), was identified by its conversion to $Cr(O^tBu)_4$ upon reaction with CuCl.

We feel that the weight of evidence indicates that only *inner-sphere* electron transfer is effective at interconverting $Cr(O^tBu)_4^-$ and $Cr(O^tBu)_4$. Thus, eq 3 would proceed through a $(^tBuO)_{4-n}Cr(O^tBu)_nLiPPh_2$ bridged species. The reaction of $Cr(O^tBu)_4^-$ with CuCl could then proceed by an analogous bridged intermediate. In fact, when CuCl is added to a blue slurry of $KCr(O^tBu)_4$ in THF, the color changes to dark brown before the blue color of $Cr(O^tBu)_4$ develops. Attempts to stabilize this brown preredox intermediate in THF by carrying out this reaction in the presence of 3 equiv of PPh_3/equiv of CuCl gave a light purple solution, which decomposed to $Cr(O^tBu)_4$ and Cu^0 over a 24-h period. When the complex formed in THF from CuCl and 2 equiv of PMe_2Ph was added to $KCr(O^tBu)_4$, the solution became deep purple (more stable than with PPh_3) but decomposed to green upon attempted crystallization.

It was observed that $KCr(O^tBu)_4$ reacts with $^1/_2$ equiv of $[Rh(COD)Cl]_2$ in either Et_2O or THF to give an intermediate yellow-green solution. The benzene-soluble component of this product ($(COD)RhCr(O^tBu)_4$?) subsequently decays to $Cr(O^tBu)_4$. Attempts to improve on this approach to an isolable inner-sphere electron-transfer intermediate are currently under way.

We have tested the hypothesis that electron transfer must occur by an inner-sphere mechanism by attempting the reduction of $Cr^{IV}(O^tBu)_4$ by the 19-valence-electron species Cp_2Co. Even at reflux temperature (9 h) in benzene there is no reaction, as indicated by persistence of the ^1H NMR signals of both reagents (Cp_2Co at −51 ppm in C_6D_6). Also unreactive are the outer-sphere reductants $Cr(CO)_6$ and $W(CO)_6$ (reflux in THF).

To summarize, the steric crowding observed in the structure of $Cr(O^tBu)_4$ accounts both for its lack of polymerization (compare smaller alkoxides) and lack of adduct formation with Lewis bases. Its observed reaction chemistry is dominated by electron transfer, but the steric shielding does not preclude alkoxide bridging to Lewis acidic redox reagents and, thus, apparent inner-sphere redox mechanisms. The ease of oxidation of $Cr(O^tBu)_4^-$ (assuming tetrahedral geometry for the CrO_4 unit) to the unusual oxidation state Cr(IV) probably originates in the relatively high energy of the t_2 HOMO in the anion.

Acknowledgment is made to the donors of the Petroleum Research Fund, administered by the American Chemical Society, to the Norwegian Research Council for Science and the Humanities, and to VISTA for support of this research.

Contribution from the Department of Chemistry, Faculty of Science, Fukuoka University, Nanakuma, Jonan-ku, Fukuoka 814-01, Japan, and Department of Electronic Chemistry, Tokyo Institute of Technology, Nagatsuta, Midori-ku, Yokohama 227, Japan

X-ray Diffraction Study of Calcium(II) Chloride Hydrate Melts: $CaCl_2 \cdot R H_2O$ (R = 4.0, 5.6, 6.0, 8.6)

Toshio Yamaguchi,*,† Shun-ichi Hayashi,‡ and Hitoshi Ohtaki‡,§

Received November 2, 1988

X-ray scattering measurements have been performed on calcium(II) chloride hydrate solutions, $CaCl_2 \cdot RH_2O$, with R = 4.0 (120 °C), 5.6 (72 °C), 6.0 (33 °C), and 8.6 (25 °C). The analysis of the radial distribution functions and model fittings revealed that in the solution of $CaCl_2 \cdot 8.6H_2O$ a Ca^{2+} ion is surrounded by six water molecules, the Ca^{2+}–OH_2 distance being 245 pm. With decreasing H_2O concentration a direct Ca^{2+}–Cl^- correlation owing to the formation of contact ion pairs appears at 270 pm. About one Cl^- ion binds to a Ca^{2+} ion in the $CaCl_2 \cdot 6H_2O$ melt, whereas about two Cl^- ions coordinate to a Ca^{2+} ion in the $CaCl_2 \cdot 4.0H_2O$ melt, whose structure is similar to that found in the crystal structure of $CaCl_2 \cdot 4H_2O$. The structure of the $CaCl_2 \cdot 6H_2O$ melt, which always yields supercooling, was investigated at 15 °C below the melting point (29.9 °C) and 80 °C. The structure in the supercooled state is similar to that found at 33 °C but different from that of $CaCl_2 \cdot 6H_2O$ crystal. A tendency of further Cl^- ion coordination to the Ca^{2+} ion with increasing temperature was observed.

Introduction

Electrolyte solutions may be classified into five categories depending on the water content according to Braunstein:[1] (I) very dilute aqueous solution, (II) concentrated aqueous solution, (III) hydrate melts, (IV) melts containing incomplete hydration sheaths, and (V) anhydrous molten salts. Most of structural studies so far reported have been devoted to categories I, II, and V. On the contrary, there appeared very few structural investigations on III and IV, in which ion–ion interactions become comparable with ion–water interactions. These solutions, which are called "hydrate melts", are of considerable interest from a structural point of view whether or not a structure change occurs through a melting/crystallization process between the solid and liquid phases. Hydrate melts are also paid attention as heat storage materials[2] in industrial applications, among which calcium(II) chloride hexahydrate[2c-f] is one of the most attractive materials from the standpoint of the melting temperature, heat storage density, and thermal stability.

The structure of concentrated aqueous $CaCl_2$ solutions classified into category II has been investigated by NMR[3] and Raman[4] spectra, self-diffusions,[5] X-ray[6] and neutron[7] diffraction, and

* To whom correspondence should be addressed.
† Fukuoka University.
‡ Tokyo Institute of Technology.
§ Present address: Coordination Chemistry Laboratories, Institute for Molecular Science, Myodaiji-cho, Okazaki 444, Japan.

(1) Braunstein, J. *Ionic Interaction (I)*; Academic Press: New York, 1971.
(2) (a) Marcus, Y. In *Molten Salt Technology*; Lovering, D. G., Ed.; Plenum: New York, 1982. (b) Gawron, K.; Schröder, J. *Energy Res.* **1977**, *1*, 351. (c) Carlsson, B.; Stymne, H.; Wettermark, G. *Sol. Energy* **1979**, *23*, 343. (d) Carlsson, B.; Wettermark, G. *Sol. Energy* **1980**, *24*, 239. (e) Bajnóczy, G.; Zöld, A. *Appl. Energy* **1982**, *10*, 97. (f) Kimura, H.; Kai, J. *Sol. Energy* **1984**, *33*, 49.
(3) Vogrin, B. F. J.; Knapp, P. S.; Flint, W. L.; Anton, A.; Highberger, G.; Malinowski, E. R. *J. Chem. Phys.* **1971**, *54*, 178.
(4) Kanno, H.; Hiraishi, J. *J. Phys. Chem.* **1983**, *87*, 3664.
(5) (a) Lyons, P. A.; Riley, J. F. *J. Am. Chem. Soc.* **1954**, *76*, 5216. (b) Hertz, H. G.; Mills, R. *J. Phys. Chem.* **1978**, *82*, 952.
(6) (a) Albright, J. N. *J. Chem. Phys.* **1972**, *56*, 3783. (b) Licheri, G.; Piccaluga, G.; Pinna, G. *J. Chem. Phys.* **1976**, *64*, 2437. (c) Licheri, G.; Piccaluga, G.; Pinna, G. *J. Am. Chem. Soc.* **1979**, *101*, 5438. (d) Caminiti, R.; Licheri, G.; Paschina, G.; Piccaluga, G.; Pinna, G. *Z. Naturforsch.* **1980**, *35A*, 1361.

0020-1669/89/1328-2434$01.50/0